Law of Mass Action, Detailed Balance, and the Modeling of Calcium Puffs

S. Rüdiger,[1] J. W. Shuai,[2,*] and I. M. Sokolov[1]

[1]*Institut für Physik, Humboldt-Universität zu Berlin, Berlin, Germany*

[2]*Department of Physics, Institute of Theoretical Physics and Astrophysics, Xiamen University, Xiamen 361005, China*

(Received 19 November 2009; published 22 July 2010)

Using deterministic-stochastic simulations we show that for intracellular calcium puffs the mixing assumption for reactants does not hold within clusters of receptor channels. Consequently, the law of mass action does not apply and useful definitions of averaged calcium concentrations in the cluster are not obvious. Effective reaction kinetics can be derived, however, by separating concentrations for self-coupling of channels and coupling to different channels, thus eliminating detailed balance in the reaction scheme. A minimal Markovian model can be inferred, describing well calcium puffs in neuronal cells and allowing insight into the functioning of calcium puffs.

DOI: 10.1103/PhysRevLett.105.048103 PACS numbers: 87.16.dj, 05.20.Dd, 05.40.−a, 87.16.dp

The assumption of well-mixedness on a given scale is crucial in many mathematical models of chemical reactions. In cellular physiology, models based on *global*, cell-averaged concentrations (reducing to systems of ordinary differential equations) reproduce, e.g., oscillations of circadian clock proteins [1]. In situations related to wave propagation in excitable media, a *local* picture is assumed leading to partial differential reaction-diffusion equations for position-dependent concentrations [2]. Both approaches rely on the mass action law. Introducing concentrations implies the existence of a domain, where molecules of all reactants are approximately homogeneously distributed. This domain must be large enough to neglect fluctuations but small compared to the length scale at which the concentrations change. Here we discuss a biochemical process on a subcellular scale, where a local concentration cannot be introduced in a useful way. Concentration gradients of one of the reactants are so steep that the assumption of mixing, here between receptor channels and their ligands, does not hold. We propose a simple representation of such reactions.

We consider localized calcium release events (puffs) associated with clusters of inositol 1,4,5-trisphosphate [IP(3)] receptor channels [3,4]. In a dual feedback loop, the channels are both stimulated and inhibited (on a slower time scale) by calcium they release from the endoplasmic reticulum (ER) [5]. The number of channels within a cluster is small and a random, stochastic opening of one of them can cause the opening of a majority of channels [6–8].

Recent high-resolution imaging [9] and computer analysis shed new light on the functionality of puffs. Reference [10] presented simulations of a cluster within realistic architecture. Because of the relatively large size of clusters [9] and rapid calcium evacuation, channels within a cluster are exposed to different calcium concentrations, thus devaluating approaches relying on mixing. We here first present a detailed computer simulation of puffs closely reproducing experimental data. The model adopts a hybrid description: While calcium concentrations are given by reaction-diffusion equations, gating transitions of channels are described within a discrete Markovian scheme. To reduce the model, we then concentrate on channels but eliminate the reaction-diffusion part by evaluating typical concentrations during release. Because of the inhomogeneous distribution of calcium, we are forced to introduce its different concentrations locally, for a direct feedback of an open channel, and at the locations of closed channels. We show that this reductional approach is capable of reproducing puffs. We further discuss that, as a consequence of imperfect mixing, the reduced model lacks detailed balance, which is a standard requirement of kinetic channel schemes. Finally, we compare characteristic properties of puff solutions to recent experiments in neuroblastoma cells.

In our simulations nine channels are placed on one surface of a cuboid [Fig. 1(a)]. Surface and cuboid represent the ER's membrane and the cytosolic space, respectively. Dynamical quantities are the concentrations of free calcium, buffers bound to calcium (dye and EGTA buffer), and the discrete states of all 36 subunits of the nine tetrameric channels. Each subunit undergoes transitions according to the standard DeYoung-Keizer (DYK) model [11]: IP(3) binding, Ca^{2+} activation binding, and Ca^{2+} inhibition binding. Transition rates between the eight subunit states were obtained by fitting experimental single channel records [12]. Details of the model and its numerical implementation can be found in the supporting material [13] and in [10,14].

Figure 1(b) shows the evolution of the number of open channels for a fixed IP(3) concentration of 0.2 μM. Channels, placed with a separation of 120 nm, open stochastically and in a cooperative manner. Accumulation of free calcium subsequently leads to inhibition of subunits and, after around 100 ms, the channels close. The duration of channel openings agrees with the duration of experimentally observed calcium puffs [9].

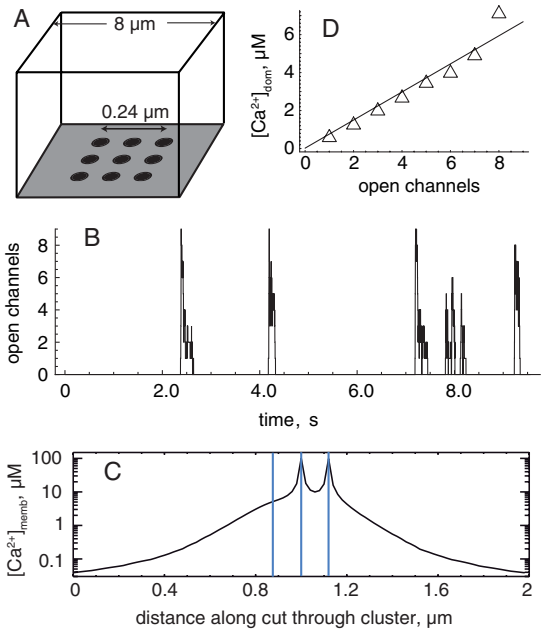

FIG. 1 (color online). Calcium release from nine channels simulated using a stochastic version of the DYK model and a deterministic reaction-diffusion scheme for Ca^{2+} and buffers. (a) The box of dimension $8 \times 8 \times 5$ μm^3 represents the cytosolic space. Channels are located in a grid on the surface (ER membrane) with calcium released into the cytosol. (b) Random puffs as cooperative openings of all or almost all channels. (c) A cut through the cluster, with vertical lines indicating the position of three channels (one is closed, two are open). (d) Calcium concentrations obtained by averaging over closed channels for a given total number of open ones.

An important open problem in the analysis of calcium signals is the determination of typical $[Ca^{2+}]$ values in the local domain of an active cluster. The magnitude of domain concentration plays a crucial role in the generation and termination of signaling events [15–18]. However, due to the properties of fluorescence imaging, the local Ca^{2+} concentrations are unclear from experimental studies, leaving the estimation of calcium levels to indirect arguments or direct numerical simulations. Recent consideration of statistical puff properties have suggested peak cluster concentrations of the order of 10 μM [18] but did not address the inhomogeneous distribution of calcium.

To determine the free calcium concentration we evaluated our direct numerical simulations and recorded $[Ca^{2+}]$ at positions of the channels. If a channel is open, large concentrations c_s of 100 μM and above are reached. However, if a channel is closed, while others are open, $[Ca^{2+}]$ assumes an intermediate value. The average of this value was defined as cluster domain concentration in [10]. Here we use a finer gradation and include the dependence of $[Ca^{2+}]$ at a closed channel on the number of open ones. If $c_i(t)$ is the Ca^{2+} concentration at the mouth of channel i at time t ($t = t_0, \ldots, t_1$) and $o_i(t)$ denotes the state of the channel (i.e., $o_i = 0$, closed; or 1, open), we define

$$c_d(n) = \sum_{i=1}^{N} \frac{1}{NT_i} \int_{t_0}^{t_1} c_i(t)[1 - o_i(t)]\delta_{nN_o(t)} dt, \qquad (1)$$

where $T_i(n) = \int_{t_0}^{t_1}[1 - o_i(t)]\delta_{nN_o(t)}dt$ is the total time when the ith channel is closed but n other channels are open, $N_o(t) = \sum_i o_i(t)$ is the number of open channels at time t, N is the total number of channels, and δ_{ij} is the Kronecker delta. The concentration $c_d(n)$ is the average concentration that a channel receives if it is closed but n other channels are open. Figure 1(d) shows that $c_d(n)$ increases linearly with n. Note that all $c_d(n)$ are considerably smaller than the concentration at the pore of an open channel (>100 μM).

Small cluster domain $[Ca^{2+}]$ results from the spatial separation of the channels and the rapid removal of calcium between the channels due to diffusion, calcium pumps, and buffer. The straight line in Fig. 1(d) represents the linear fit

$$c_d(n) = c_0 + c_1 n, \qquad (2)$$

with $c_0 = 0.02$ μM and $c_1 = 0.74$ μM. Thus, our approach leads to a large $[Ca^{2+}]$, $c_{s,0} \approx 120$ μM, for channel self-coupling and to smaller values $c = c_d(n)$ for the coupling to other channels. For calcium release from a cluster we cannot assume that reactants [IP(3)R channels and Ca^{2+}] are well mixed in the domain, since channels do not diffuse in the considered time scales [19] and the distribution of calcium ions is inhomogeneous. Therefore, the usual assumption of mass action kinetics breaks down and we are forced to consider the case of $c_s \neq c_d$ in the reaction scheme if we want to use a channel population model to discuss puff dynamics.

We further found that $[Ca^{2+}]$ values in the cluster equilibrate to c_s and c_d within milliseconds of openings or closings. We therefore consider a reduced model, in which $[Ca^{2+}]$ is given by $c_{s,0}$ and Eq. (2) but the Markovian evolution of channel states is retained. This corresponds to a coarse graining on the cluster scale and adopting different Ca^{2+} concentrations in different domains.

We first show that, due to the scale separation, the ensuing reaction scheme does not have to obey detailed balance. According to the DYK model, each channel has four subunits; each of them can bind activating and inhibiting Ca^{2+} [we ignore the IP(3) dynamics for brevity]. The state of a channel can be denoted by a four digit number, where each digit represents one of the four subunits. Each digit, in a bitwise fashion, takes on either 0 (no Ca^{2+} bound), 1 (activating Ca^{2+} bound), 2 (inhibiting Ca^{2+} bound), or 3 (both activating and inhibiting). In total there are $4^4 = 256$ states connected by transition arrows. A channel opens if at least three subunits are in state 1. Any event of binding of calcium to an open channel (e.g., the open state 0111) should be determined by the spike calcium value c_s, whereas other Ca^{2+}-binding transitions are determined by $c = c_d(n)$. Figure 2 shows a part of the transition lattice involving the open state 0111 and a

loop. Evaluating the product of rates in the clockwise and counterclockwise loop, one finds that the condition $a_5 c_d a_2 c_s b_5 b_2 = a_2 c_d a_5 c_d b_2 b_5$ necessary for detailed balance is trivially satisfied if $c_d = c_s$, but it does not hold if separation of calcium scales is assumed. We note here that the absence of detailed balance in the reduced theory is due to its coarse-grained character and represents the fact that the local equilibrium at a channel position does not correspond to a global one [20]. Invalidity of the mass action law is reflected by the two different binding rates $a_2 c_s$ and $a_2 c_d$ in Fig. 2(a), which should be contrasted with the linear rate $a_2 c$ in earlier models with detailed balance.

Figure 2(b) shows that the reduced model generates puffs of cooperated release reminiscent of the experimentally observed puffs and the puffs in our full model. What is the relevance of breaking detailed balance? To answer this question we will describe simulations with the reduced model and compare it with simulations in a related DYK model, which obeys detailed balance. Under the latter condition, we let

$$c_s(n) \equiv c_d(n) = c_0 + c_1 \frac{n}{N_{\max}}(c_{s,0} - c_0), \qquad (3)$$

which gives rest level concentration c_0 if all channels are closed, the self-coupling value $c_{s,0} = 120\ \mu M$ if all channels are open, and a linear dependence on open channel numbers. Here, we have assumed that c_1, which is a rescaled form of the parameter c_1 in Eq. (2), equals 1. In the following, however, c_1 will be a free parameter of the model.

In accordance with the estimate of cluster sizes in neuroblastoma cells in [9], we performed simulations for clusters with 5 to $N_{\max} = 10$ channels. Leaving all parameters in the determination of calcium concentrations c_d and c_s unchanged amounts to generally smaller maximal calcium concentrations for a cluster with fewer channels. For instance, a cluster of five channels where all channels are open reaches the same c_d value as a cluster of nine channels with five open channels. This treatment corresponds to keeping the cluster diameter fixed at 240 nm.

We have first calculated the distribution of peak amplitudes of puffs [Fig. 3(a)]. For these curves we have determined the maximal number of open channels during each of the events such as those in Fig. 2(b). We have first studied the case of broken detailed balance. For all channel numbers we found a strongly bimodal distribution, with many blips (single channel openings) and maximal puffs, which incorporate all of the available channels. Figure 3(b) shows a weighted average of the distributions for 5–10 channels exhibiting a peak of P_n at $n = 5$ channels. Comparison with experimental results (bars) shows good agreement in the overall distribution for puffs. However, we obtained many more blips than in the experiments (data not shown), which may be due to a higher temporal resolution, that was fixed to 1 ms in our analysis.

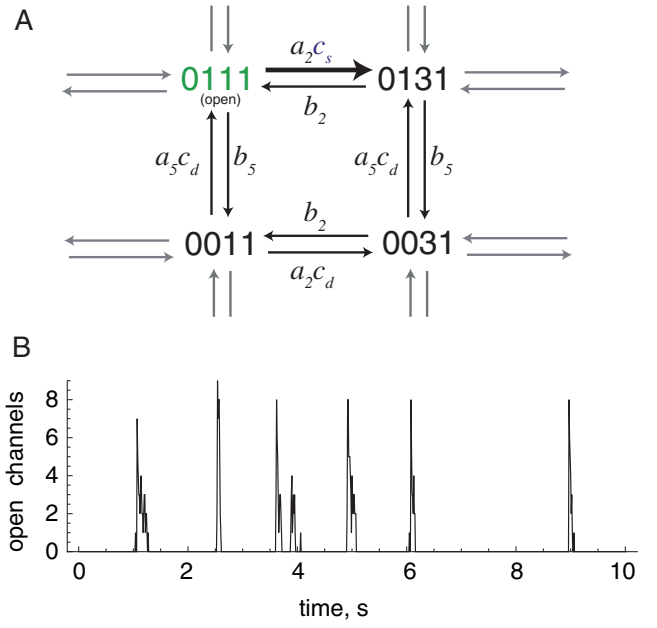

FIG. 2 (color online). (a) Exemplary loop in the transition lattice of the DYK model. Because of the separation of Ca^{2+} concentration scales, different $[Ca^{2+}]$ values appear on opposite sides of some loops involving open states. As a consequence, a net flux in the direction of the thick arrow is generated. (b) Puffs in the reduced model, where transitions are given by the DYK scheme and calcium concentrations $c_s = c_{s,0}$ and c_d given by Eq. (2).

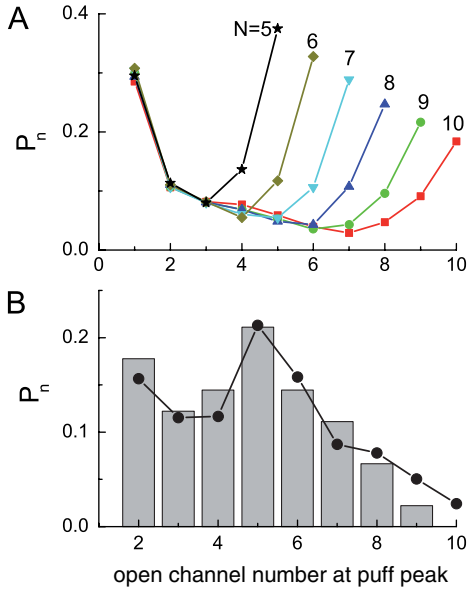

FIG. 3 (color online). (a) The distribution of puff peak amplitudes for clusters with $N = 5$–10 channels using the reduced model under conditions of broken detailed balance. Graphs in (b) are weighted averages of data as in (a). Simulations with 5–10 channels were weighted based on the experimental distribution of channels per cluster (Fig. 4C in Ref. [9]). For comparison, bars present experimental data from Fig. 4D in Ref. [9] (blips have been omitted from this analysis).

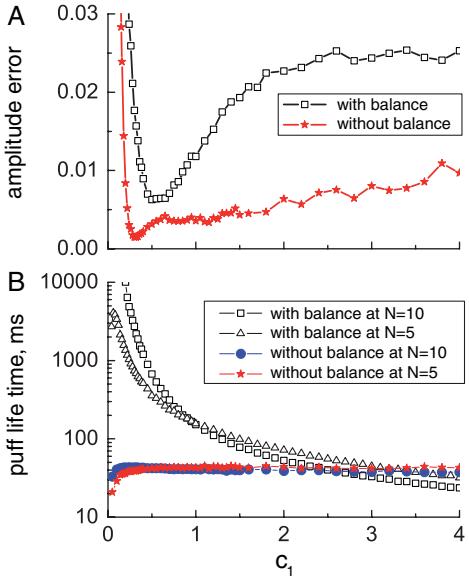

FIG. 4 (color online). (a) The deviation from the experimental puff amplitude distribution [bars in Fig. 3(b)] was calculated for models with and without detailed balance using the error sum $\sum_{i=2}^{10}(P_n - P_{n,\mathrm{exp}})^2$. (b) The puff lifetime (average for events with more than one channel opening) is constant over a large range of parameter c_1 for the broken detailed balance model (circles and stars). For models with Eq. (3) realistic lifetimes can be achieved for c_1 larger than 1 only (see open boxes and triangles), which implies increased binding site concentrations c_s larger than 120 μM.

We next compared our model with models obeying detailed balance by fitting them to experimental data of two of the best studied puff properties. Our goal was an optimum for varying the parameter c_1 in Eqs. (2) (broken balance) and (3) (balance). The parameter c_1 represents the effective separation of channels and depends, for instance, on the concentration of mobile buffer [10]. Figure 4 shows the models' errors in peak distributions [difference between bars and dots in Fig. 3(b)] and puff lifetime. Puff lifetime has been obtained as full duration at half maximum and should be compared to experimental values of around 50 ms [9]. The best agreement can be found for the case of broken detailed balance for c_1 around 0.3. However, for the model (3) it is impossible to obtain both short puffs and a realistic amplitude distribution for the same parameter value c_1.

In summary, we have described how the standard coarse-graining approach fails for strongly localized biochemical processes. An assumption of well-mixedness does not hold since concentration gradients of reactants are very steep. For a correction, we suggest to separate concentration scales into large open channel values and smaller concentrations at closed channels. We obtain a reduced Markovian model, which replicates temporal spikes in the reaction very well. Importantly, the scale separation leads to a breakdown of detailed balance on the coarse-grained level of channel gating models. By comparison of our results with experimental data we identified the relevance of breaking the detailed balance. First, in order to fit the patch clamp data for isolated channels [12], inhibition occurs at large Ca^{2+} concentrations (dissociation constant $d_2 = 50\ \mu M$, see supporting material [13]). For a model with detailed balance, however, cluster domain concentrations are too small for inhibition if c_1 is small, resulting in too long puffs. On the other hand, if c_1 is large ($c_1 > 2$), one can find short puffs, but now c_s is large already for small numbers of open channels, effectively suppressing large amplitude puffs. This problem does not occur in models with broken detailed balance, which provide two different Ca^{2+} scales for puff activation and termination. Therefore, our approach facilitates the robust generation of short puffs with large peak amplitudes. These results are crucial in understanding localized calcium signals, which are a basic part of many cellular signaling processes, for instance, in neurons or muscle cells.

S. R. and I. S. acknowledge support from the DFG within program SFB 555. J. S. has been supported by the NSF China under Grant No. 10775114 and the NIH U.S. under Grant No. 2RO1GM065830-06A1.

*jianweishuai@xmu.edu.cn

[1] J. Keener and J. Sneyd, *Mathematical Physiology: Cellular Physiology* (Springer, New York, 2008).
[2] B. Pando, J. E. Pearson, and S. P. Dawson, Phys. Rev. Lett. **91**, 258101 (2003).
[3] I. Parker, J. Choi, and Y. Yao, Cell Calcium **20**, 105 (1996).
[4] R. Thul and M. Falcke, Phys. Rev. Lett. **93**, 188103 (2004).
[5] M. Bär *et al.*, Phys. Rev. Lett. **84**, 5664 (2000).
[6] S. Swillens *et al.*, Proc. Natl. Acad. Sci. U.S.A. **96**, 13 750 (1999).
[7] J. W. Shuai and P. Jung, Phys. Rev. Lett. **88**, 068102 (2002).
[8] M. Falcke, Adv. Phys. **53**, 255 (2004).
[9] I. F. Smith and I. Parker, Proc. Natl. Acad. Sci. U.S.A. **106**, 6404 (2009).
[10] S. Rüdiger *et al.*, Biophys. J. 99, 3 (2010).
[11] D. W. DeYoung and J. Keizer, Proc. Natl. Acad. Sci. U.S.A. **89**, 9895 (1992).
[12] J. W. Shuai *et al.*, Chaos **19**, 037105 (2009).
[13] See supplementary material at http://link.aps.org/supplemental/10.1103/PhysRevLett.105.048103 for a description of model and numerical methods.
[14] S. Rüdiger *et al.*, Biophys. J. **93**, 1847 (2007).
[15] G. Ullah and P. Jung, Biophys. J. **90**, 3485 (2006).
[16] G. Ullah, P. Jung, and K. Machaca, Cell Calcium **42**, 556 (2007).
[17] H. DeRemigio, J. R. Groff, and G. D. Smith, Math. Med. Biol. **25**, 65 (2008).
[18] D. Swaminathan, G. Ullah, and P. Jung, Chaos **19**, 037109 (2009).
[19] I. F. Smith *et al.*, Sci. Signal. **2**, ra77 (2009).
[20] V. Nguyen, R. Mathias, and G. D. Smith, Bull. Math. Biol. **67**, 393 (2005).